

Insulation Performance and Microstructure in Modified Polyethylene by MPE

X. Wang,¹ D. M. Tu,¹ C. Lei,² Q. G. Du²

¹State Key Laboratory of Electrical Insulation and Power Equipment, Xi'an Jiaotong University, Xi'an 710049, China

²The Key Laboratory of Molecular Engineering of Polymer, Fudan University, Shanghai 200433, China

Received 16 November 2006; accepted 3 April 2007

DOI 10.1002/app.26735

Published online 11 September 2007 in Wiley InterScience (www.interscience.wiley.com).

ABSTRACT: Electrical measurements have shown to be able to provide useful information on physical, chemical, and microstructural properties of dielectric material. In this article, the depolarization characteristics of low-density polyethylene blended with a small amount of metallocene catalyzed polyethylene were measured by pulsed electro-acoustic method under various stresses. According to space charge limited current theory, the derivation of quantities such as mean volume density of space charge, apparent trap-controlled mobility, trap depth distribution, and threshold stress were discussed. The test results showed that low-density polyethylene blended with 1 wt % metallocene catalyzed polyethylene could effectively decrease deep trap density, increase shallow trap density, and then improve the mobility of charges. We also meas-

ured the breakdown voltage and tensile strength of the blends. It was found that low-density polyethylene blended with a small amount of metallocene catalyzed polyethylene could effectively improve its breakdown voltage and tensile strength but reduce the material tenacity. Finally, mechanical relax and crystalline morphology of blends were studied by dynamic mechanical measurement, wide-angle X-ray diffraction, and small-angle X-ray scattering experiments. The results showed that the improvement of electrical properties and mechanical strength in the blends were relevant to the crystalline morphology. © 2007 Wiley Periodicals, Inc. *J Appl Polym Sci* 107: 21–29, 2008

Key words: polyethylene; charge transport; breakdown; morphology; mechanical property

INTRODUCTION

Low density polyethylene (LDPE) has excellent electrical and mechanical properties, and it is widely used to produce crosslinked polyethylene power cables. As these cables are used at high voltages and large currents, the insulation of power cables are required to have superior electrical properties of volume resistivity, breakdown strength, space charge accumulation, and better mechanical behaviors. Now, many researchers have committed to the modification of polyethylene to improve its dielectric properties.^{1–4} Among these, blending LDPE with other polymers is a convenient and an effective way to improve the breakdown strength of LDPE. To avoid a microscopic inhomogeneity formed at boundary of two different components which can influence the dielectric properties of the blends, the best way of blends is to use two such kinds of components that their chemical structures are similar. There were some researches about PE blends of high-density polyethylene and LDPE to enhance

breakdown behavior, because of the modification of the local lamellar texture, but mechanism of change in breakdown behavior was far from clear.^{5,6}

In our previous work,⁷ a small amount of metallocene catalyzed polyethylene (MPE) was used to blend with LDPE at a content of MPE below 5 wt %. MPE was selected because of its good compatibility with LDPE. Then the effects of MPE in the blends on the dielectric properties and crystalline morphology of LDPE were investigated on film specimens. We found that LDPE blended with a small amount of MPE could not only increase crystallization temperature and crystallinity, but also decrease spherulites' size and the perfect degree of crystallization, especially in LDPE blended with 1 wt % MPE. And at the same time, the test results of dielectric properties showed that LDPE blended with 1 wt % MPE had a least volume resistivity, a highest direct current (DC) breakdown strength, and less space charge accumulation. Polyethylene is a typical semicrystalline polymer. The improvement of dielectric properties of the blends was probably attributed to the morphological changes by blending, namely, the decrease of spherulites' size and the form of imperfect spherulites.

Dielectric properties of polymer are relevant to its physical, chemical, and microstructural properties.^{8–10} On the basis of our previous work,⁷ the charge trans-

Correspondence to: D.M. Tu (dmtu@mail.xjtu.edu.cn).

Contract grant sponsor: National Science Foundation of China (Project Nos. 59777001, 50577008).

port properties in the blends were investigated by pulsed electro-acoustic (PEA) method in this article. And then, according to space charge limited current (SCLC) theory, the derivation of quantities such as mean volume density of space charge, apparent trap-controlled mobility, trap depth distribution, and threshold stress were obtained expressly. At the same time, the tensile strength and mechanical relax mechanism were studied by mechanical property test. Finally, the breakdown and X-ray tests further indicated the relationship between the crystalline morphology and electrical breakdown. So, the aim of this article was expected to link the microstructure (molecule motion, crystallization) with macrostructure (tensile strength, dielectric properties) in the polymer.

EXPERIMENTAL

Materials and specimen preparation

LDPE is a cable grade product of Daqin 18D type, and its density is about 0.917 g/cm^3 . The trademark of MPE is EXACT 0203 from Exxon Mobile Chemical Company and its density is about 0.902 g/cm^3 . LDPE and MPE (1, 3, 5 wt %, respectively) were mixed in a Brabender Plasticorder at a rotor speed of 60 rpm and a temperature of 120°C for 5 min. The pure LDPE was subjected to the same process to be used as a reference. The LDPE/MPE blends and pure LDPE were respectively, pressed to boards and films at 120°C for 10 min as the test specimens. The size of board specimens is about $14 \text{ cm} \times 20 \text{ mm} \times 5 \text{ mm}$, and the size of films is about $10 \text{ cm} \times 10 \text{ cm} \times 0.4 \text{ mm}$. Before measurement, all film specimens were heat-treated at 80°C for 8 h. So, the effects of crystalline morphology induced by stress and cooling rate could be eliminated during the compression process of films.

Charge transport properties

The depolarization characteristics of the film specimens were measured by the PEA¹¹ method under various stresses (2.5–50 kV/mm) for 2 h. According to SCLC theory,¹² the derivation of quantities, such as mean volume density of space charge, apparent trap-controlled mobility, trap depth distribution and threshold stress, were discussed.

DC prevoltage and opposite-polarity breakdown test

The direct current (DC) prevoltage and opposite-polarity breakdown voltage was measured by the needle-plate electrode configuration. Sharpened sewing needles having a radius of curvature of about

$5 \mu\text{m}$ at the tip of the needles were carefully selected for the needle electrodes. The needle was cleaned with alcohol and then dried in a vacuum oven. After this cleaning process, an array of 10 needles, acting as high voltage (HV) electrode, were inserted by means of a puncher into the board specimen which had been heated at a temperature of 80°C for about 20 min. The spacing between the needles was 10 mm and the electrode gap between the needle and plate was 2.5 mm. The plate, acting as the ground electrode, was formed by the surface of the specimen with conductive medium. Then the specimens and electrodes were immersed into the silicon oil to avoid the breakdown of air. The initiative DC voltage of 30.8 kV was applied on the needle electrode of specimens through $4 \text{ M}\Omega$ resistance, and then an equivalent transient opposite-polarity voltage was applied in each 3 min for 40 times. Subsequently, the DC voltage was increased with a step of 1.4 kV and the earlier-mentioned process was repeated until the specimen was breakdown.

Small-angle X-ray scattering and wide-angle X-ray diffraction experiments

A D/max-rB diffractometer (Rigaku, Japan) equipped with a $\text{CuK}\alpha$ tube and Ni filter was employed to investigate the crystallinity of the film specimens over a range of diffraction angle $2\theta = 10\text{--}40^\circ$. Small-angle X-ray scattering experiments were performed on Rigaku D/max-RB scattometer (Rigaku, Japan) using $\text{CuK}\alpha$ radiation ($\lambda = 0.154 \text{ nm}$) with a scanning range of $2\theta = 0.2\text{--}2.8^\circ$.

Dynamic mechanical properties

The dynamic mechanical spectrum of film specimens from -150°C to 100°C was investigated by a dynamic mechanical spectrometer (PE-7). The test frequency was 1 Hz, and the temperate was increased at the rate of $3^\circ\text{C}/\text{min}$.

Tensile strength test

The tensile experiment on dumbbell film specimens with a thickness of about 0.4 mm was done by CMT type tensile machine. The tests were performed five times under the same experimental condition, and the average values of tensile strength and breaking elongation ratio were calculated.

RESULTS AND DISCUSSION

Charge transport properties

Electrical measurements have shown to be able to provide useful information on physical, chemical,

and microstructural properties of dielectric material. So, the change of trap density by chemical-physical modification will result in the change of charge injection and transport properties.¹³ In fact, space charge accumulation rate and extent is associated to interfaces (electrode-dielectric, crystalline-amorphous), defects, contaminants, additives, and, hence, to technological process, as crosslinking, blending, mixing additives, which are often carried out to improve or modify material characteristics.¹⁴ The extracted quantities, i.e., threshold for space charge accumulation, rate of charge accumulation as function of field, apparent mobility, trap density, and trap depth distribution should be logically sensitive to the earlier material features.^{15,16}

Mean volume density of space charge

Figure 1 shows charge distributions in specimens applied under stress of 50 kV/mm for 2 h followed by short-circuiting for 30 s. It is obviously observed that there remain a lot of remnant space charges in specimens and has a least amount in LDPE blended with 1 wt % MPE. It is also seen from Figure 1 that there are obvious homogenous electron injections at electrode, but the hole injection is inconspicuous because the barrier of electron injection from electrode is lower than that of hole. The injection of

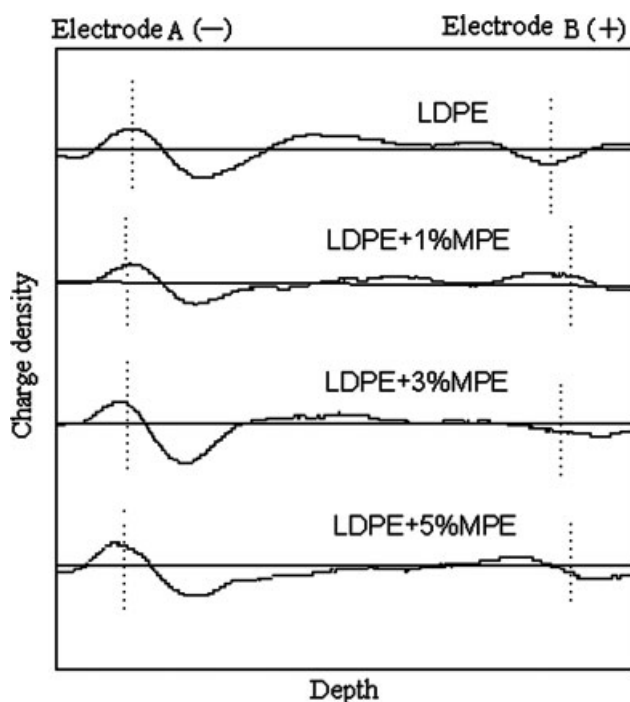


Figure 1 Space charge profiles during depolarization in specimens applied under a stress of 50 kV/mm for 2 h followed by short-circuiting for 30 s.

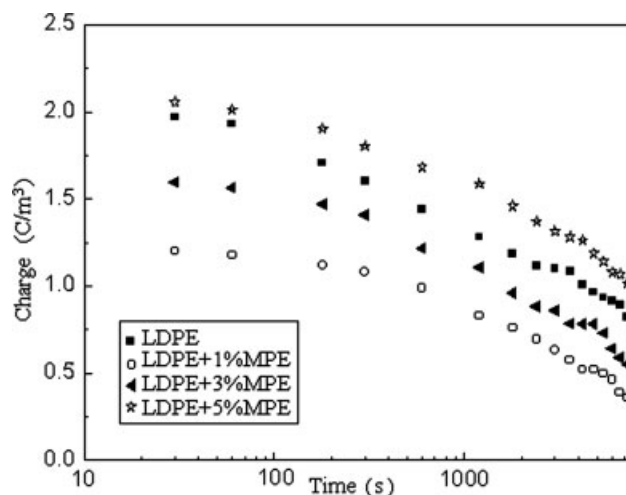


Figure 2 Depolarization characteristic in specimens applied under stress of 50 kV/mm for 2 h followed by short-circuiting.

charge is almost restrained and the remnant charge is the least in bulk when the content of MPE is equal to 1 wt %. This means that LDPE blended with 1 wt % MPE not only decreases the space charge in bulk, but also improves the surface state of specimen so as to restrain the injection of homogenous charge from electrode.

When the specimens are under stress for a given time (polarization) and then are short-circuited (depolarization), charge dynamic observed by PEA are damping gradually during depolarization and the mean volume density of space charge at time t can be calculated from the space charge profiles by using the following expression:

$$Q(t; E_p) = \frac{1}{L} \int_0^L |Q_p(x, t; E_p)| dx \quad (1)$$

where, $Q(t; E_p)$ is the total charge in the specimen at time t of depolarization, E_p is poling stress, Q_p is the charge detected at time t in insulation section x , 0 and L denote the electrode positions.

Neglecting charge injection and recombination at high stress,¹⁷ we measure the charge profile in MPE/LDPE blends under prestressed 50 kV/mm for 2 h and then short-circuited for different time (from 30 to 7200 s). Accordingly, depolarization characteristic determined according to Eq. (1) is reported in Figure 2.

It is noteworthy that the remnant space charges of each specimen reduce gradually with the increase of depolarization time, and they have a least value at any depolarization time when the content of MPE is equal to 1 wt % and increase again with the increase of MPE contents. It is well-known that the remnant

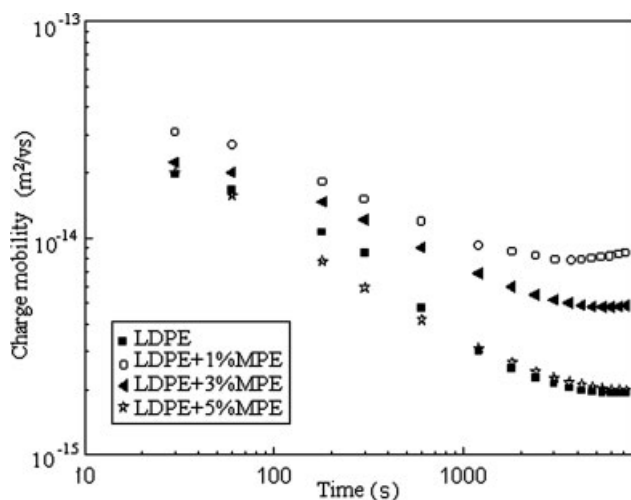


Figure 3 Apparent trap-controlled mobility as a function of depolarization time.

charges are related to the depth or density of traps. The deeper or higher density the traps are, the more charges accumulate under stress.

Apparent trap-controlled mobility

The depolarization process is the trapped charge detrapping from the traps. Neglecting charge recombination at high stress, we can obtain apparent trap-controlled mobility relevant to charge detrapping through the measurement of depolarization characteristic of polymer. According to Poisson equation and simplified models of the charge continuity, we assume that the charge damping is due to leak current, the prevailing charge is unipolar and located close to electrodes, the simplest expression of trap-controlled mobility is obtained as follow¹⁸:

$$\mu(t) = \frac{2\varepsilon}{Q(t)^2} \frac{dQ(t)}{dt} \quad (2)$$

where, $Q(t)$ is the charge density that can be calculated, according to Eq. (1), at any depolarization time, and dQ/dt is the slope of the depolarization curve at time t . The earlier-mentioned expression derived from conduction current measurements describes prevalently shallow trap behavior, since shallow traps are mostly involved in conduction process.

Figure 3 shows the apparent trap-controlled mobility by Eq. (2) through fitting the depolarization curve. As can be seen, the mobility has a maximal value in LDPE blended with 1 wt % MPE and is damping slowly with the time. However, the mobility of blends decreases gradually with the increase

of MPE contents and is close to pure LDPE when the content of MPE is equal to 5 wt %.

Apparent trap-controlled mobility, varying with depolarization time, is related to charge releasing from deeper and deeper traps as polarization time increases. The report in Ref. 7 shows that LDPE blended with 1 wt % MPE can not only effectively decrease spherulites' size and the depth of traps, but also increase the charge mobility. The effect of MPE versus LDPE is comprised of two parts. On the one hand, according to nucleation, MPE can reduce decrease spherulites' size so as to decrease the depth of traps. On the other hand, its own many branched chains result in new traps and try to increase depth of trap in LDPE. Both aspects are paradox to form space charge. So, the new traps in LDPE induced by the branched chains of MPE increase with the increasing MPE contents, resulting in the decrease of charge mobility and the accumulation of many charges. Combining Figures 2 and 3, we can see that LDPE blended with 1 wt % MPE has the fastest mobility and the least remnant charges. This is attributed to the formation of shallow traps.

Trap depth distribution

According to SCLC, Italy, Prof. Montanari built a new model for trap depth evaluation.¹³ It is shown that the total number of charges trapped in the specimen at time t can be expressed, under the assumption of discrete distribution of trap levels, by:

$$n_{\text{TOT}}(t) = \sum_{i=2}^m n_i(t) = \sum_{i=2}^m a_i \exp(-b_i t) \quad (3)$$

where,

$$a_i = n_i(0) \quad (4)$$

$$b_i = v \exp\left(\frac{\Delta U'_i}{kT}\right) \quad (5)$$

$$\Delta U'_i = U'_i - U'_1 \quad (6)$$

$n(i)$ is the number density of charges trapped in the i th lever, m is the total number of levels, with potential energy decreasing from level 1 to level m , $v = kT/h$ is the attempt frequency, T is temperature, h is Planck constant, and $U'_i - U'_1$ is the activation energy between levels i and 1. The total charge trapped in the specimen at time t , $n_{\text{TOT}}(t)$, namely $Q(t)$, can be approximately measured by space charge observation, through Eq. (1), once the nature of charge carriers is known. Hence, the depolarization characteristic can be used to estimate the coefficients a_i and b_i of Eq. (3) and thus, the trap depth distribution $\Delta U'_i$.

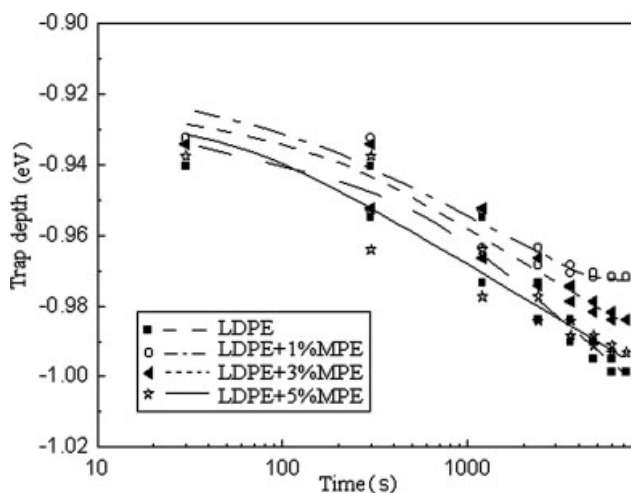


Figure 4 Trap depth distribution as a function of depolarization time.

Figure 4 shows the distribution of trap depth in specimens calculated by Eq. (3). It is noteworthy that the charges detrapp gradually from shallow traps to deep traps. In general, for polymer insulation, the trap depth less than 1.10 eV is thought as shallow trap. Moreover, the trap depths shown in Figure 4 are all below than 1.0 eV, which proves again that only shallow traps relevant to conduction current can be measured. It is also seen from Figure 4 that the trap depth of LDPE with 1 wt % MPE obviously decrease, compared with pure LDPE. Then the trap depth gradually increases with the increase of MPE contents and exceeds pure LDPE when the content of MPE is equal to 5 wt %. It is remarkable that the trap depth of LDPE with 5 wt % MPE is higher than pure LDPE when short time less than 5000 s, and less than pure LDPE when short time more than 5000 s. It is a wonder whether the defects or new traps energy formed by branched chains of MPE approximately distribute over -0.94 to -0.98 eV.

Threshold stress

According to SCLC theory, the conduction current of material include three regions such as Ohm, SCLC, and filled trap.¹² The concept of threshold is the voltage or field at which the Ohm region turns to SCLS region, namely, is the minimum field, about which charge begins to accumulate in insulation.¹⁶

The slope of curve in SCLS region indicates the rate of charge accumulation.^{12,19} In general, working at electric stresses below the threshold means extremely long life and reliability in service. So, detection of the threshold and rate at which space charge is accumulated is useful for insulation characterization even if the threshold value is not employed as a design reference.

According to Eq. (1), plotting:

$$q_{s0} = q_s(E, t_0) \quad (7)$$

where $t_0 = 30$ s is a reference depolarization time as a function of poling field, the so-called threshold characteristic is obtained. This is a source of interesting quantities that can be correlated with material physical-chemical and microstructural properties, i.e., the threshold for space charge accumulation and the slope b .^{12,15,16,20}

Figure 5 reports the space charge threshold characteristics for the blends prestressing under different stress for 2 h and then short-time for 30 s. It can be seen that the threshold for space charge increases significantly when the content of MPE is equal to 1 wt % and decreases again with the increase of MPE contents. The threshold fields are about 12, 20, 17, and 13 kV/mm for pure LDPE, LDPE blended with 1% MPE, 3% MPE, and 5% MPE, respectively. It is also seen that the slope b of each specimen is basically same, this means that LDPE blended with a small amount of MPE never changes the rate of charge accumulation in PE.

DC pre-voltage and opposite-polarity breakdown voltage

The DC pre-voltage and opposite-polarity breakdown voltage measured by the needle-plate electrode configuration depends on the stress at the tip of needle. When the needle is negative-polarity voltage, the needle electrode injects electrons, and then forms high opposite-polarity field when the instant opposite-polarity voltage is applied. Subsequently, the breakdown of dielectric occurs. But, because the injection of hole is harder than that of electron, the opposite-polarity breakdown voltage of sample with positive-polarity needle is higher than that with negative-polarity needle.

Figure 6 shows the DC pre-voltage and opposite-polarity breakdown voltage under positive and negative field. It can be seen that the 50% opposite-polarity breakdown probability of negative-polarity is lower than that of positive-polarity, and all blends have a higher breakdown voltage than pure LDPE, whether the polarity of applied voltage is positive or negative. The breakdown voltage has a maximal value when the content of MPE is equal to 1 wt % and reduces with the increase of MPE contents. According to the earlier-mentioned analysis of trap depth, LDPE blended with a small amount of MPE can effectively decrease the trap depth and increase charge mobility in PE, thereby, avoiding the accumulation of charges at the tip of needle and increasing the breakdown strength.

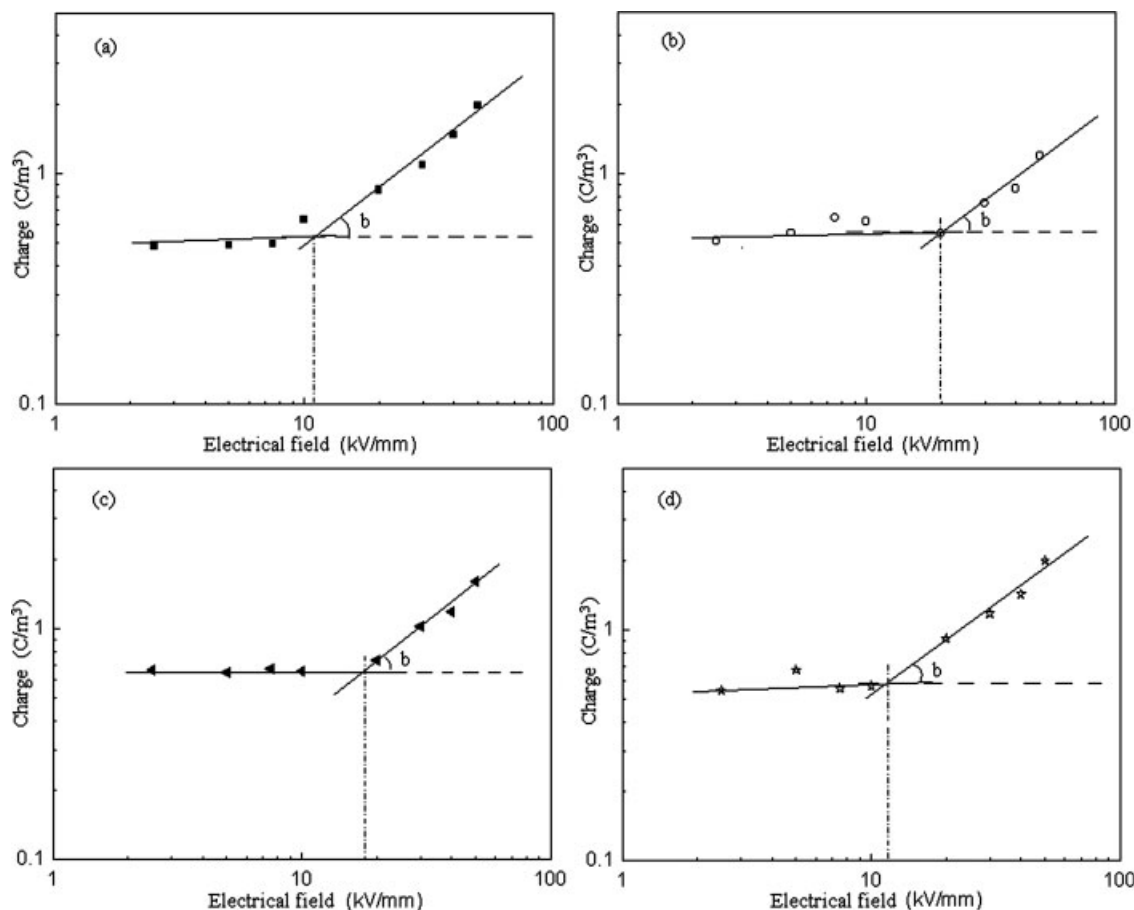


Figure 5 Threshold stress of charge injection. (a) LDPE; (b) LDPE + 1% MPE; (c) LDPE + 3% MPE; (d) LDPE + 5% MPE.

Crystallinity and weight-average long period

Polyethylene is a typical semicrystalline polymer, including crystalline phase and amorphous phase. The weight-average long period (L_B) of lamellar morphology can be calculated from the peak position q_{\max} of scattering vector in the Figure 7 revised by Lorentz method.²¹ Then, on the basis of Bragg's equation and mathematic formula of scattering vector, the weight-average long period can be obtained from the following equation.

$$L_B = 2\pi/q_{\max} \quad (8)$$

$$q = \frac{4\pi \sin(2\theta/2)}{\lambda} \quad (9)$$

where, θ is scattering angle, λ is the wavelength of the light source.

The long period L_B is the parameter representing the density change of crystalline and amorphous regions. Table I shows the long period of blends calculated from earlier-mentioned equation. It can be seen that the addition of MPE decreases the long period of PE slightly and the long period of the blends

has a least value when the content of MPE is equal to 1 wt %. Lamella thickness L_c and amorphous thickness L_a can be obtained from the following formula:

$$L_c = L_B \times X_c \quad (10)$$

$$L_a = L_B(1 - X_c) \quad (11)$$

where, X_c is the crystallinity of polymer, which can be got from the following wide-angle X-ray diffraction (WAXD) test.

The three peaks because of the crystalline phase appear in WAXD patterns of specimens as shown in Figure 8. The peaks in the diffractions are appeared at 2θ of 21.4° , 23.7° , 36.1° corresponding to the 110, 200, 020 lattice planes of orthorhombic crystalline form of polyethylene, respectively. The amorphous phase is shown near 2θ of 19.8° as a broad peak. No monoclinic or triclinic form's refraction is found in X-ray patterns. These results show that LDPE blended with a small amount of MPE does not change the crystalline form. Suppose X-ray diffraction strength is just relevant to crystalline and amorphous phases, then, the crystallinity X_c can be denoted as the percent of crystalline part. So, through

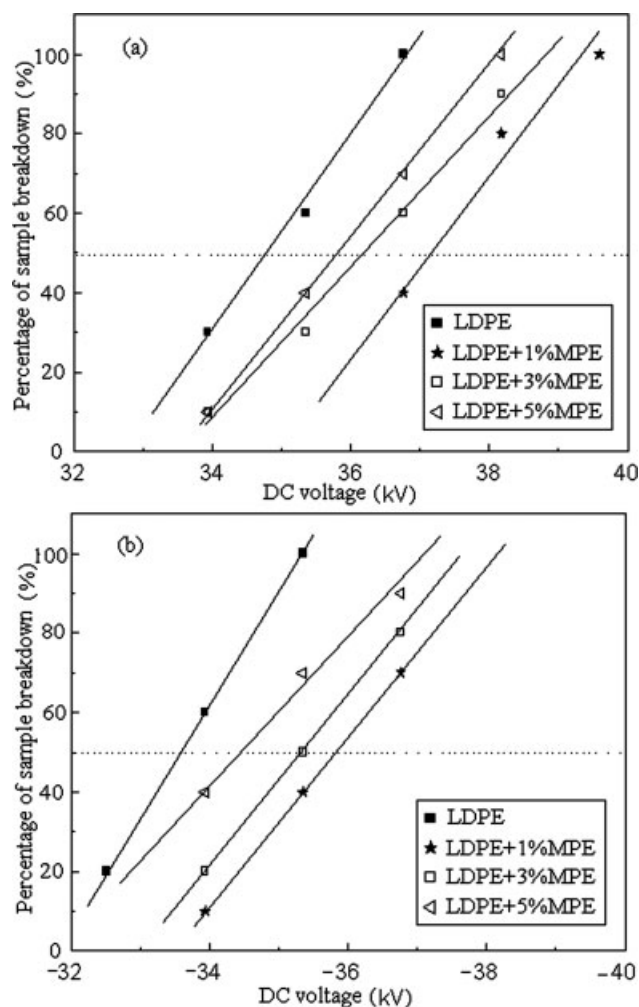


Figure 6 Relationship between DC pre-voltage and opposite-polarity breakdown ratio in the blends. (a) positive-polarity pre-voltage; (b) negative-polarity pre-voltage.

the modification of diffraction strength of each crystal plane by numerical fitting and separation of peak method and the calculation of integral area of each diffraction strength, crystallinity X_c shown in Table I can be got from Eq. (12).

$$X_c = \frac{I_{110} + 1.42I_{200}}{I_{110} + 1.42I_{200} + 0.75I_a} \in [0, 1] \quad (12)$$

It is found from Table I that the long periods of all blends decrease, and lamella thickness increases or amorphous thickness decreases in the blends. Generally, the carrier trap and charge hopping site in PE are located at the amorphous phase or the interface of crystalline phase and amorphous phase, such as defect, void, oxide, etc. The electrical breakdown path mainly passes through amorphous area in polymers, and then path advances along the boundaries of spherulites, or trans-crystal, or lamella.¹⁹ So, the

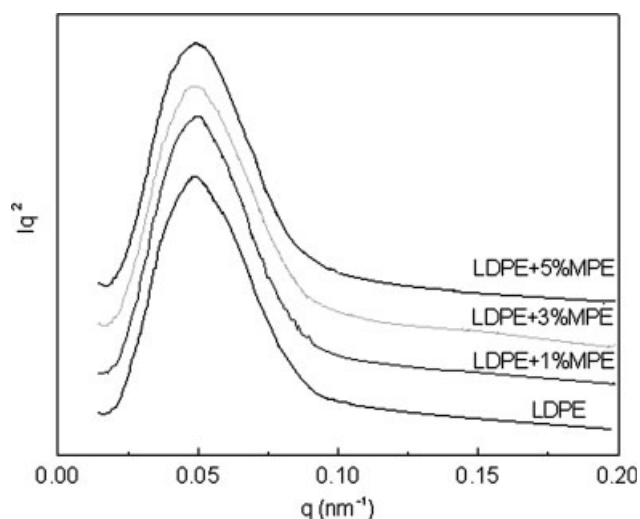


Figure 7 Lorentz-corrected SXAS profiles of the blends.

increase of breakdown strength of the blends is attributed to the increase of lamella thickness and the decrease of amorphous thickness in PE.

Dynamic mechanical properties

Figure 9 shows the dynamic mechanical properties of the blends. The report in Ref. 22 shows that γ peak is the relaxation of 3–5 CH_2 crankshaft motional unit, β peak is the relaxation of long branched chain in amorphous phase, α peak is the relaxation of motional unit in crystalline phase. It can be seen from Figure 9 that LDPE blended with a small amount of MPE can effectively improve the storage modulus (E') at the range of lower temperature (below 0°C). It is attributed to the increase of crystallinity of the blends that results in the improvement of strength and stiffness. At the same time, α peak and γ peak are obvious but β peak is ambiguous in all specimens. The appearance of α peak indicates that the imperfect crystalline forms in the blends and little change of α peak width of blends show great compatibility. α peak in LDPE blended with 1 wt % MPE transferring to higher temperature (from 56°C up to 62°C) indicates that

TABLE I
Crystalline Morphology of Specimen from WAXD and SAXS

	LDPE	LDPE + 1% MPE	LDPE + 3% MPE	LDPE + 5% MPE
Long period (\AA)	130	122	124	126
Lamella thickness (\AA)	44	55	52	50
Amorphous thickness (\AA)	86	67	72	76
Crystallinity (%)	34	45	41	39

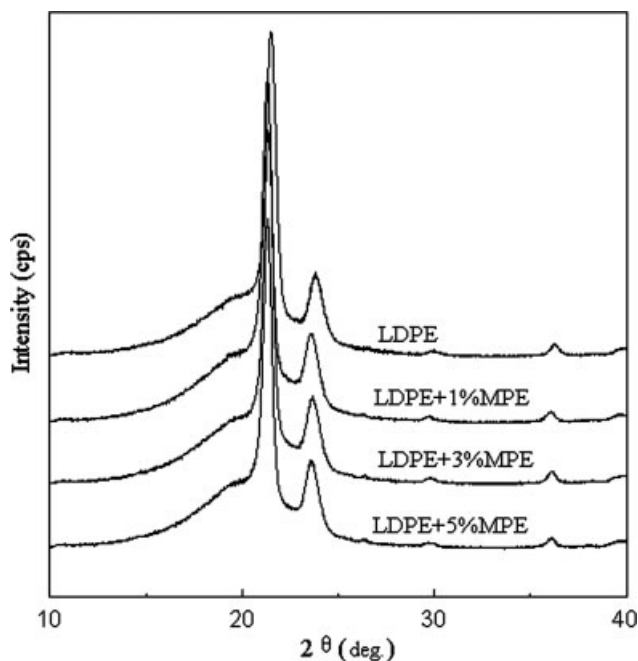


Figure 8 WAXD diffractograms of the blends.

the increase of lamella thickness or crystallinity improves the interaction of intermolecular and then restricts the motion of molecular. The ambiguous β peak shows the less long branched chains in amorphous phase or is drowned by α strong peak. Otherwise, γ peak of blends has little change, compared with pure LDPE.

Tensile strength

Figure 10 shows the curve of tensile property. It is noteworthy that the addition of MPE to LDPE can improve tensile strength but decrease tenacity, to some extent. It is well known that the tensile strength and breaking elongation ratio of polymer are relevant to its crystallinity. The increase of crystallinity can improve the intermolecular force in polymer, and then increase the tensile strength and decrease breaking elongation ratio because of the embrittlement of specimen.

Furthermore, in semicrystalline polymers, when polymer is applied to a high electrical field, an electron has to traverse amorphous and crystalline regions that behave differently with respect to the transport mechanism. Crystalline regions have a resistivity to charges because the molecular chains array in a compact and orderly manner. In contrast, amorphous regions have a strong affinity for charges not only because chains array in a loose and disorderly manner, but also all the impurities (including free radical residuals, peroxides, ions, and double bonds) almost disperse in amorphous phase, especially in the defects and the interfaces of spherulites.

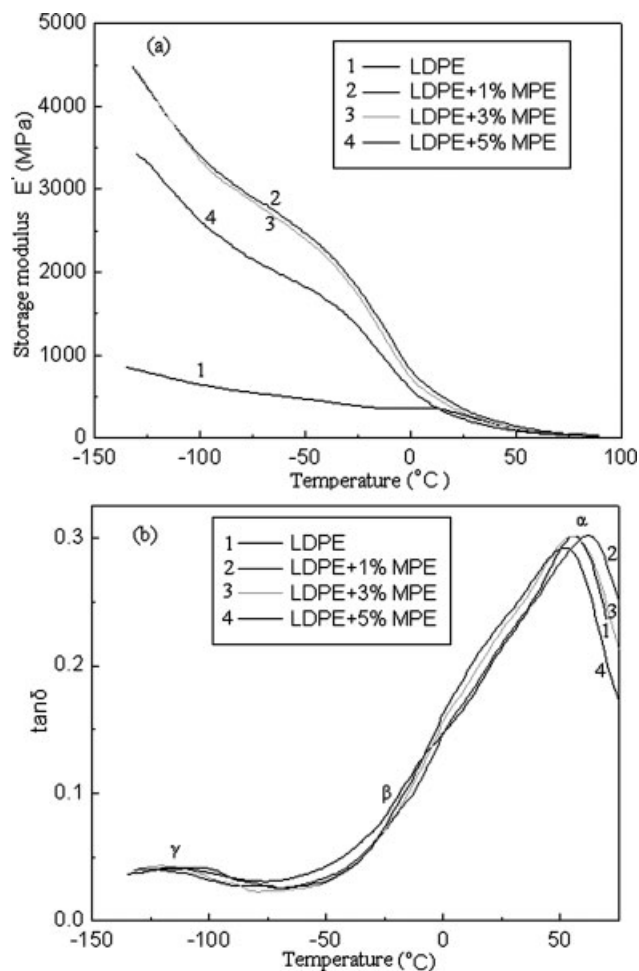


Figure 9 The DMA spectra of the blends. (a) storage modulus; (b) mechanical loss.

Meanwhile, amorphous regions constitute the continuous phase in which the random chain can pass the charges on to the neighbor chain by changing its configuration. Hence, the dielectric properties may

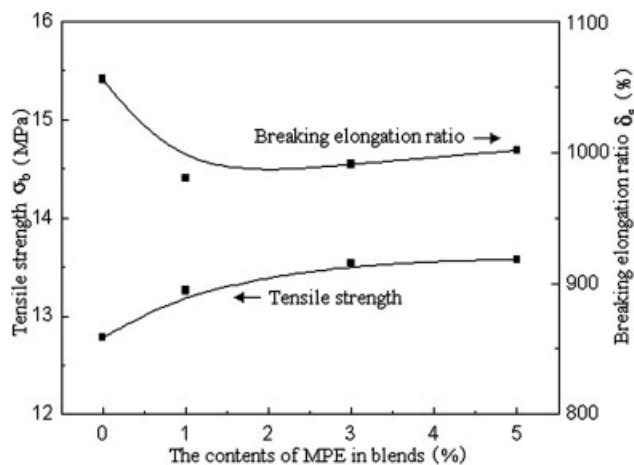


Figure 10 Influence of the content of MPE on the tensile strength and breaking elongation ratio in the blends.

depend strongly on the microstructure of the polymeric morphology.

The results of the PEA method indicate that the improvement of mobility or threshold stress and the decrease of depth of traps in blends are attributed to the forms of many shallow traps which make charges travel the entire material freely and reduce the charge accumulation in a partial locality. And at the same time, the decrease of trap depth and the increase of charge mobility avoid the accumulation of charges at the tip of needle electrode so as to improve the DC prevoltage and opposite-polarity breakdown voltage. It is well known that breakdown strength is related to the crystallinity. The higher crystallinity is, the less amorphous phase exists and then the higher breakdown strength is. The paper in Ref. 19 also indicates that the electrical breakdown path advances along the boundaries of spherulites, or *trans*-crystal, or lamella of LDPE. This means that electrical breakdown path passes through amorphous area in polymers. The analysis of crystalline morphology by WAXD, small-angle X-ray scattering, and DMA tests all indicate the increase of crystallinity that results in the increases of breakdown voltage and the tensile strength. In conclusion, the form of shallow traps and the increase of crystallinity improve the breakdown voltage, crystal size, storage modulus, and tensile strength. This also validates that the relationship between the microstructure and macrostructure in the polymer again.

CONCLUSIONS

In this article, we have investigated the relationship between micro-properties (molecule motion, crystalline morphology, and charge migration) and macro-properties (tensile strength and breakdown voltage) in LDPE blended with a small amount of MPE. The following conclusions may be drawn from the analysis:

1. PEA test results show that LDPE blended with 1 wt % MPE can effectively decrease the density of deep traps and increase the density of shallow traps. At the same time, the charge mobility and threshold stress in blends are improved too.
2. The decrease of trap depth and the increase of charge mobility avoid the accumulation of charges at the tip of needle electrode so as to improve the DC prevoltage and opposite-polarity breakdown voltage.
3. WAXD and small-angle X-ray scattering test results show that the increase of breakdown voltage in blends is also attributed to the

decrease of the weight-average long period and the increase of crystallinity (i.e., the increase of crystal size and the decrease of amorphous region) which restrains the development of electrical breakdown path.

4. DMA test results show that both polyethylenes have great compatibility. The increase of crystallinity not only improves the storage modulus, but also makes α peak in LDPE blended with 1 wt % MPE transfer appreciably to higher temperature.
5. The increase of crystallinity of the blends improves the interaction of intermolecular, accordingly improving the tensile strength. However, the breaking elongation ratio is decreased due to the embrittlement of specimen.

References

1. Tanaka, Y.; Chen, G.; Zhao, Y.; Davies, A. E.; Vaughan, A. S.; Takada, T. IEEE Trans Dielectr Electr Insul 2003, 10, 148.
2. Salah Khalil, M.; Cherfi, A.; Toureille, A.; Reboul, J. P. IEEE Trans Dielectr Electr Insul 1996, 3, 743.
3. Suh, K. S.; Kim, J. Y.; Noh, H. S.; Lee, C. R. IEEE Trans Dielectr Electr Insul 1995, 2, 1.
4. Suh, K. S.; Yoon, H. G.; Lee, C. R.; Okamoto, T. IEEE Trans Dielectr Electr Insul 1999, 6, 282.
5. Martin, C. P.; Vaughan, A. S.; Sutton, S. J. Annu Rep Conf EIDP 2003, 1, 309.
6. Hosier, I. L.; Vaughan, A. S.; Swingler, S. G. J Polym Sci Part B: Polym Phys 2000, 38, 2309.
7. Wang, X.; Wu, C. Y.; Tu, D. M. IEEE Proc 8th ICPADM 2006, 1, 139.
8. Gao, L. Y.; Guo, W. Y.; Tu, D. M. IEEE Trans Dielectr Elec Insul 2003, 10, 233.
9. Gao, L. Y.; Tu, D. M.; Zhou, S. C.; Zhang, Z. L. IEEE Trans Dielectr Electr Insul 1990, 25, 534.
10. Li, X.; Cao, Y.; Du, Q.; Yin, Y.; Tu, D. M. J Appl Polym Sci 2001, 82, 611.
11. Li, Y.; Yasuda, M.; Takada, T. IEEE Trans Dielectr Electr Insul 1994, 1, 188.
12. Montanari, G. C. IEEE Trans Dielectr Electr Insul 2000, 7, 309.
13. Mazzanti, G.; Montanari, G. C.; Palmieri, F. IEEE Trans Dielectr Electr Insul 2003, 10, 198.
14. Montanari, G. C. IEEE Trans Dielectr Electr Insul 2004, 11, 56.
15. Mazzanti, G.; Montanari, G. C.; Alison, J. M. IEEE Trans Dielectr Electr Insul 2003, 10, 187.
16. Montanari, G. C.; Fabiani, D. IEEE Trans Dielectr Electr Insul 2000, 7, 322.
17. Teyssedre, G.; Laurent, C.; Montanari, G. C.; Palmieri, F.; See, A.; Dissado, L. A.; Fothergill, J. C. J Phys D: Appl Phys 2001, 34, 2830.
18. Montanari, G. C.; Mazzanti, G.; Palmieri, F.; Bertuzzi, B. IEEE Proc 8th ICPADM 2000, 1, 38.
19. Yamamoto, Y.; Ikeda, M.; Tanaka, Y. IEEE Trans Dielectr Electr Insul 2004, 11, 881.
20. Montanari, G. C.; Laurent, C.; Teyssedre, G.; Campus, A.; Nilsson, U. H. IEEE Trans Dielectr Electr Insul 2005, 12, 438.
21. Chiu, H. J.; Chen, H. L.; Lin, J. S. Polymer 2001, 42, 5749.
22. Sethi, M.; Neeraj, K.; Gupta, K.; Srivastava, A. K. J Appl Polym Sci 2002, 86, 2429.